

# Cinchona Alkaloid–Metal Complexes: Noncovalent Porous Materials with Unique Gas Separation Properties\*\*

Janusz Lewiński,\* Tomasz Kaczorowski, Daniel Prochowicz, Teodozja Lipińska, Iwona Justyniak, Zbigniew Kaszukur, and Janusz Lipkowski

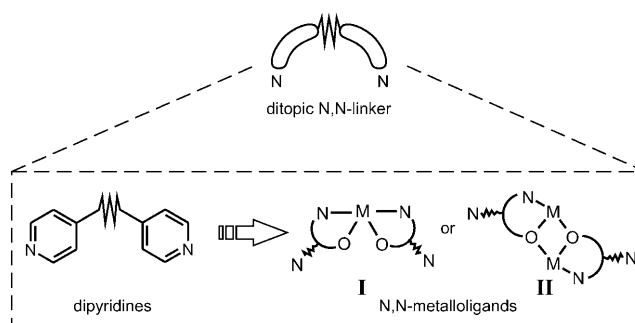
Dedicated to Professor Stanisław Pasynekiewicz on the occasion of his 80th birthday

A particularly demanding task in the area of hybrid organic–inorganic materials has been the engineering of well-defined void nanospaces<sup>[1]</sup> capable of selectively binding a guest molecule to perform a specific function of the system, such as catalysis,<sup>[2]</sup> storage,<sup>[3]</sup> or separation.<sup>[4]</sup> The most common and effective approach to design and prepare metal–organic frameworks (MOFs) or porous coordination polymers (PCPs) of desired topology and functionality is based on coordination-driven self-assembly, and both the correct choice of metal centers and the engineering of the ligand's features, such as size, flexibility, and directionality of binding centers, play a decisive role.<sup>[5]</sup> An additional level of tailorability in the design of these hybrid materials can be achieved by implementation of metalloligands.<sup>[5c,6]</sup>

Alternatively, soft noncovalent synthesis from simple molecular metal complex-based building blocks could provide a convenient and economic way to construct noncovalent porous materials (NPMs) with a unique guest-responsive framework,<sup>[1f,7]</sup> and this approach is one of the major challenges in chemistry. Molecular metal complexes are potentially very attractive as building units for microporous architectures, as relatively weak intermolecular bonding interactions in these supramolecular structures allow the microcavities to conform to the shape or functionality of the guest molecules. However, construction of robust NPMs based on this alternative strategy is still in its infancy and examples of such materials are very rare,<sup>[8]</sup> which stems from

the inherent propensity of molecular crystals to form architectures of maximal density.<sup>[9]</sup>

Recently, we have been focusing on rational design strategies to replace common bipyridines as N-ditopic organic linkers<sup>[10]</sup> by metal complexes with pyridyl units, namely cinchonine-based metalloligands. Initially we synthesized bischelate aluminum complexes,  $XAl(CN)_2$  (where CN = deprotonated cinchonine), as novel chiral N,N-metalloligands **I** (Scheme 1), and demonstrated their excellent capability as



Scheme 1. Strategy for developing novel N-ditopic linkers.

metallotectons for noncovalent-interaction-driven self-assembly into novel microporous chiral architectures prone to enantioselective sorption, as well as their coordination-driven self-organization for constructing coordination polymers of helical topology.<sup>[11]</sup> Herein, we extend this strategy to dinuclear aluminum–cinchonine complexes as novel molecular building blocks **II** to produce flexible homochiral NPMs. We show that the resulting NPMs can compete with classical MOFs as highly selective adsorbents exhibiting unique properties, such as temperature-triggered adsorption as well as very high affinities for  $H_2$ ,  $CO_2$ , and  $CH_4$ .

A dimethylaluminum derivative of cinchonine,  $[Me_2Al(\mu-CN)]_2$  (**I**), was prepared in high yield by the addition of 1 equiv of  $AlMe_3$  to a slurry of cinchonine (CN-H) in THF (Scheme 2; for experimental details see the Supporting Information). We note that the synthesis and spectroscopic characterization of **I** was reported previously and the variable-temperature  $^1H$  NMR studies revealed that it exists in solution as a dimeric five-coordinate adduct of formula  $[Me_2Al(\mu-CN)]_2$  with a relatively high activation energy ( $80.8 \text{ kJmol}^{-1} \text{ K}^{-1}$ ) for the dissociation of the Al–N dative bond.<sup>[12]</sup> As structural details for  $[R_2Al(\mu-CN)]_2$  complexes were still lacking,<sup>[13]</sup> as well as being encouraged by the above-

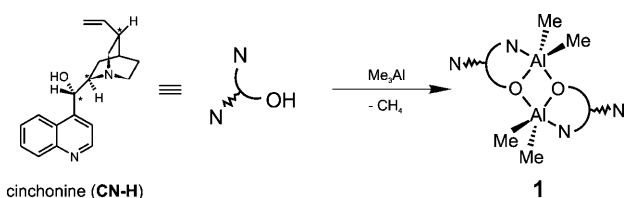
[\*] Prof. Dr. J. Lewiński, T. Kaczorowski, D. Prochowicz  
Department of Chemistry, Warsaw University of Technology  
Noakowskiego 3, 00664 Warsaw (Poland)  
Fax: (+48) 22-234-7279  
E-mail: lewin@ch.pw.edu.pl  
Homepage: <http://lewin.ch.pw.edu.pl>

Prof. Dr. J. Lewiński, Dr. I. Justyniak, Dr. Z. Kaszukur,  
Prof. Dr. J. Lipkowski  
Institute of Physical Chemistry, Polish Academy of Sciences  
Kasprzaka 44/52, 01224 Warsaw (Poland)

Dr. T. Lipińska  
Institute of Chemistry, University of Podlasie  
3 Maja 54, 08110 Siedlce (Poland)

[\*\*] We thank Dr. W. Bury for experimental assistance during gas adsorption measurements. This work was supported by the Ministry of Science and Higher Education (grants N N204 and PBZ-KBN-117/T08/06).

Supporting information for this article is available on the WWW under <http://dx.doi.org/10.1002/anie.201002925>.



**Scheme 2.** Synthesis of the metalloligand.

mentioned results for the monomeric  $XAl(CN)_2$ -type complexes,<sup>[11]</sup> we put a lot of effort into obtaining single crystals of the title compounds suitable for X-ray diffraction studies. We succeeded when THF was used as the crystallization solvent.

The molecular and crystal structures of **1**·THF are shown in Figure 1a and Figure 1S in the Supporting Information.<sup>[14]</sup> The dimeric structure of **1** possesses  $C_2$  symmetry with two five-coordinate aluminum centers and displays basic geometric parameters typical for this type of dialkylaluminum alkoxide.<sup>[15]</sup> The geometry of the Al atom coordination sphere can be described as a distorted trigonal bipyramid with the axial positions occupied by the alkoxide oxygen atom and the quinclidine nitrogen atom (the average intramolecular Al–N distance is 2.216 Å). The quinoline moieties are oriented in nearly parallel fashion with the N atoms 8.61 Å away from each other, and the links of the potential N,N-ditopic linker form an angle of 49.3°.

Noncovalent-interaction-driven self-assembly of **1** leads to a homochiral three-dimensional (3D) network with one-dimensional (1D) channels filled by THF molecules (Figure 1c and Figure 1S in the Supporting Information). A detailed analysis of this supramolecular architecture shows that assembly of single molecules of **1** results in the formation of an array of crystallographically equivalent two-dimensional (2D) bilayer sheets stacked along the *c* axis by van der Waals interactions. The two sublayers that define the bilayer motif are connected by a combination of intermolecular C–H···N hydrogen bonds and C–H··· $\pi$  interactions (Figure 2S in the Supporting Information). The interaction between a quinclidine hydrogen atom and a quinoline nitrogen atom (with the C–H···N distance of 2.63 Å) from separate **1** units

produces a set of parallel 1D hydrogen-bonded chains within a single sublayer. Additionally, a network of intermolecular C–H··· $\pi$  interactions involving another quinclidine C–H bond pointed towards the homocyclic ring of a quinoline system (with the closest C–H··· $\pi$  distance of 2.84 Å) interweaves the pair of sublayers, thus facilitating the formation of the bilayer structure.

Most notably, the layers are crossed perpendicularly by a set of homochiral 1D open channels filled by THF molecules. Each single-pore column is formed by separated **1** molecules arranged in a left-handed helical pattern (a “virtual helix” with a pitch of 17.5 Å), with uncoordinated quinoline N donors positioned in the vicinity of others from adjacent **1** units (Figure 1b and Figure 2S in the Supporting Information). In view of the potential gas adsorption properties of **1** (see below), those nitrogen atoms are hardly accessible from the inside of the channels, as indicated from the analysis of the crystal packing. The “virtual helices” are further organized into a porous superstructure by interdigitation with four neighboring helices, by utilizing **1** units and gaps between them as tongues and grooves (Figure 2S in the Supporting Information). A more thorough inspection of the shape of the solvent-excluded pore reveals a high curvature of the Connolly surface (Figure 1b and Figure 1S in the Supporting Information), with a channel diameter varying from 3.0 Å in the neck region to 5.2 Å in the widest section.<sup>[16]</sup> These values classify the system as an ultramicroporous material.

Thermogravimetric analysis of **1**·THF showed that THF can be removed from the porous structure by heating to 100°C (Figure 3S in the Supporting Information). This process leads to an approximate 10% weight loss of the system, which corresponds to a 1:1 ratio of  $[Me_2Al(\mu-CN)]_2$  per encapsulated THF molecule, in agreement with the single-crystal data. Variable-temperature powder X-ray diffraction (PXRD) studies (Figure 7S in the Supporting Information) clearly revealed that **1** retains its crystallinity after removal of the solvent molecules (50°C under dynamic vacuum) and, surprisingly, preserves the values of the unit cell parameters with only a minor increase of a monoclinic cell angle ( $\beta$  angle increases from 91.4 to ca. 95°).<sup>[14]</sup> A comparison of the PXRD pattern (21–23°C) with that calculated on the

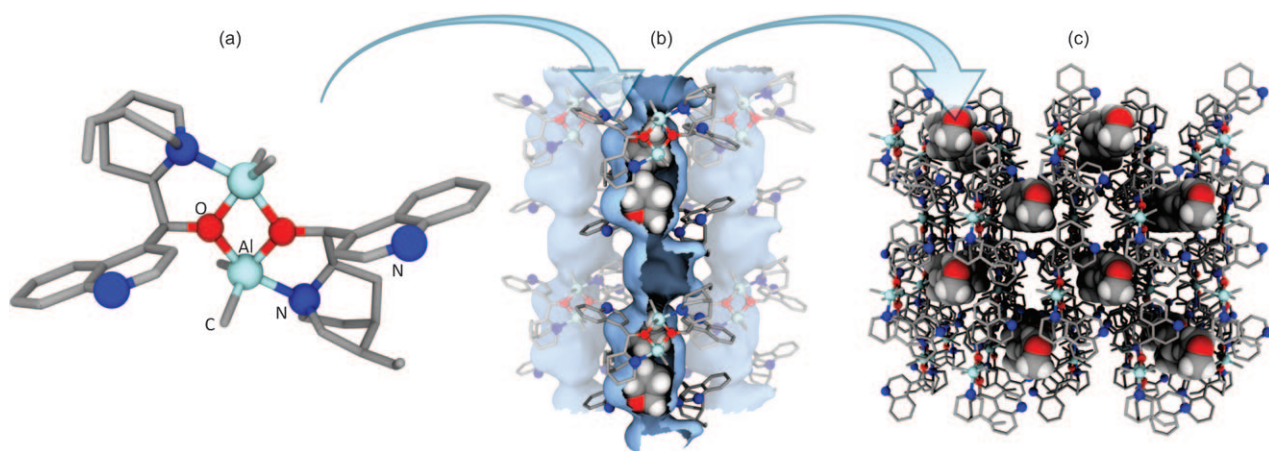


**Figure 1.** Self-organization process of the metalloligand **1** into a NPM with homochiral 1D open channels filled by THF molecules.

basis of the single-crystal data reveals moderate changes in the peak intensities that can be attributed to the noncovalent framework flexibility and slight structural modifications upon solvent loss. Increasing the temperature causes anisotropic lattice expansion (with maximum expansion along the *b* axis) followed by framework collapse at about 70 °C.

The permanent porosity of the solvent-free structure of **1** was further verified by gas sorption experiments using N<sub>2</sub>, H<sub>2</sub>, CH<sub>4</sub>, and CO<sub>2</sub>. At 77 K, **1** takes up H<sub>2</sub> molecules (kinetic diameter of 2.89 Å) with a type I isotherm typical of microporous materials, with an uptake of 0.54 wt % (61.0 cm<sup>3</sup>g<sup>-1</sup> at standard temperature and pressure (STP), see Figure 2a). A marked hysteresis observed in the adsorption–desorption cycle could be an effect of both the ultramicropore dimensions and the highly corrugated surface, which hinder diffusion of H<sub>2</sub> molecules through the pore apertures. This interpretation is further supported by a significantly heightened initial isosteric heat of adsorption (*Q*<sub>st</sub>) value of 11.9 kJ mol<sup>-1</sup> (Figure 4S in the Supporting Information).<sup>[17]</sup> To our knowledge, the observed value is the highest reported so far for the adsorption of H<sub>2</sub> on an NPM sample, and is of the same order of magnitude as that for MOFs with modified

internal surfaces (the heat of adsorption in classical MOFs lies in the range of 3.5–6.5 kJ mol<sup>-1</sup>,<sup>[3b,18]</sup> and for MOFs with modified internal surfaces can increase to 10–13.5 kJ mol<sup>-1</sup><sup>[19]</sup>). Being unable to measure the Brunauer–Emmett–Teller (BET) surface area from N<sub>2</sub> adsorption experiments (see below), we evaluated the value of 125 m<sup>2</sup>g<sup>-1</sup> from the H<sub>2</sub> (77 K) adsorption isotherm. Thus, the H<sub>2</sub> uptake (0.54 wt %) of desolvated **1** at 1 bar is remarkably high for a material with such a modest BET surface area.<sup>[3b]</sup>

Surprisingly, attempts to evaluate an N<sub>2</sub> adsorption isotherm at 77 K revealed no significant uptake up to 1 bar (Figure 2a), thus indicating the presence of gated voids in the host framework which block diffusion of N<sub>2</sub> molecules (kinetic diameter of 3.64 Å) across the channel network. This observation falls into line with the above-mentioned micropore size in **1** (ca. 3.0 Å in the neck). Strikingly, at 195 K the pore apertures open to accommodate a moderate amount of N<sub>2</sub> (18.0 cm<sup>3</sup>g<sup>-1</sup> at STP, 0.6N<sub>2</sub> per formula unit). We believe that this temperature-triggered adsorption effect can be attributed to the kinetically controlled flexibility of **1**, in which at higher temperatures large-amplitude lattice vibrations induce dynamic local frame distortions resembling peristaltic motions that facilitate diffusion of guest molecules.<sup>[20]</sup> Such an explanation seems to be consistent with the observation that oversized THF molecules can be evacuated from the ultramicropores of **1** without loss or change of the host structure.<sup>[21]</sup> Increasing the N<sub>2</sub> adsorption temperature to 273 K diminishes the adsorbent–adsorbate interactions, which results in minimal N<sub>2</sub> uptake under STP conditions (Figure 2c).

The unique sorption properties of the discussed NPM are further exemplified by significant CO<sub>2</sub> and CH<sub>4</sub> uptakes at 195 K (Figure 2b) in spite of their different shape and character (CO<sub>2</sub> has a permanent quadrupole moment, unlike CH<sub>4</sub>), as well as kinetic diameters (3.3 and 3.8 Å, respectively) larger than that of the effective pore window. The storage capacities at 1 bar amount to 13.8 wt % (70.5 cm<sup>3</sup>g<sup>-1</sup> at STP) and 2.0 wt % (28.0 cm<sup>3</sup>g<sup>-1</sup> at STP) for CO<sub>2</sub> and CH<sub>4</sub>, respectively. The isosteric heats of adsorption (Figures 5S and 6S in the Supporting Information) have zero-coverage values of 35.7 (CO<sub>2</sub>) and 24.8 kJ mol<sup>-1</sup> (CH<sub>4</sub>). These values indicate strong interactions of the adsorbate molecules with the pore walls at low pressures and are significantly higher than typical initial adsorption values for classical MOF materials.<sup>[22]</sup>

Recent reports clearly demonstrate that decoration of the MOFs' internal surfaces with amine groups significantly enhances interactions with CO<sub>2</sub>.<sup>[22a,23]</sup> Note then that uncoordinated quinoline nitrogen atoms of **1** units could potentially account for the high *Q*<sub>st</sub> value for CO<sub>2</sub>, yet they are inaccessible to adsorbate molecules as evidenced from the crystal structure. Still, one could imagine that the dynamic motions of **1** molecules in the soft crystal framework allow for temporal exposition of quinoline nitrogen atoms into the adsorption area. The other factor responsible for the high *Q*<sub>st</sub> values may be the undulating shape of the ultramicropores that seems to be a direct source of van der Waals pocket sites, that is, the areas of potential overlap that would strengthen

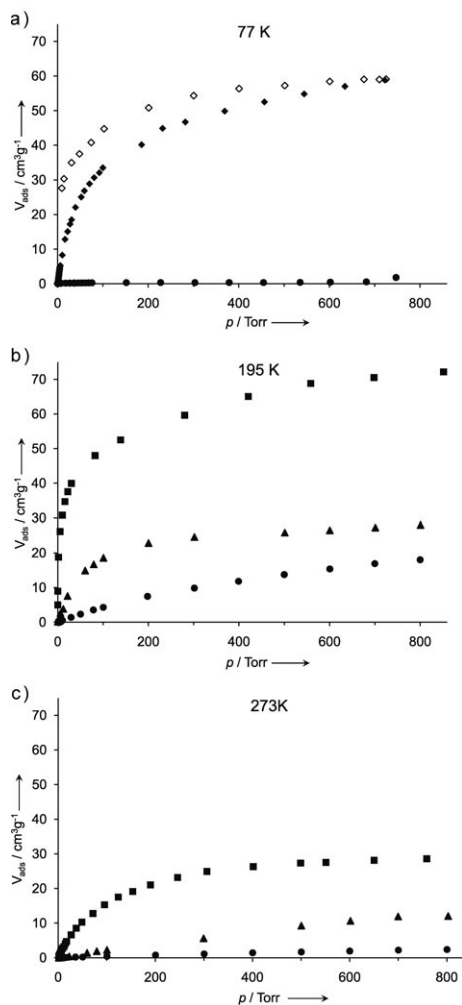


**Figure 2.** H<sub>2</sub> (◆), N<sub>2</sub> (●), CO<sub>2</sub> (■), and CH<sub>4</sub> (▲) adsorption isotherms for **1** at a) 77, b) 195, and c) 273 K; open symbols denote desorption.

the affinity of **1** to CO<sub>2</sub>, as well as serve as primary adsorption locations for CH<sub>4</sub> molecules.<sup>[22a]</sup> The micropore volume estimated from the Dubinin–Radushkevich equation for CO<sub>2</sub> adsorption data at 273 K equals approximately 0.16 cm<sup>3</sup> g<sup>-1</sup>, which is close to the values of 0.181 and 0.174 cm<sup>3</sup> g<sup>-1</sup> obtained on the basis of PLATON<sup>[24]</sup> and Materials Studio calculations, respectively. The BET surface area evaluated from CO<sub>2</sub> adsorption data at 273 K is 147 m<sup>2</sup> g<sup>-1</sup> and corresponds to that calculated from H<sub>2</sub> adsorption data.

The adsorption behavior of **1** demonstrated by the isotherms indicates that the title NPM material stands as an exciting device for gas separation that utilizes its flexible porous structure for highly selective sorption of H<sub>2</sub> and CO<sub>2</sub> over N<sub>2</sub> in the corresponding temperature ranges. Its operation is based on either a size-exclusion mechanism at low temperatures (H<sub>2</sub>/N<sub>2</sub> at 77 K) or host–guest interaction-driven equilibrium separation at higher temperatures (CO<sub>2</sub>/N<sub>2</sub> at 273 K). The corresponding selectivities at low pressures were estimated<sup>[23a]</sup> to be about 28:1 for H<sub>2</sub>/N<sub>2</sub> separation at 77 K and 74:1 for CO<sub>2</sub>/N<sub>2</sub> separation at 273 K. To our knowledge, the latter selectivity value is among the best reported to date for MOF materials.<sup>[23a]</sup>

In conclusion, we have demonstrated that dinuclear alkylaluminum–cinchone complexes can effectively act as molecular building units, and provide a viable means for constructing new chiral microporous architectures through noncovalent-interaction-driven self-assembly. By following the presented strategy, we obtained a novel flexible noncovalent ultramicroporous material with a 1D pore system that shows unique structural and gas separation properties. Desolvation of **1**·THF occurs with preservation of the crystal structure parameters to form an effective molecular sieve at low temperatures and a selective host–guest interaction-directed adsorbent at higher temperatures. Switching of the mode of operation is achievable by temperature control of the framework's flexibility, which enables diffusion of oversized guests through micropores resembling breathing or peristaltic-like motions. Moreover, **1** exhibits strong H<sub>2</sub>, CH<sub>4</sub>, and CO<sub>2</sub> binding with initial enthalpies of adsorption of 11.9, 24.8, and 35.7 kJ mol<sup>-1</sup>, respectively, which are significantly larger than the corresponding typical value ranges for classical MOFs. We believe that the reported approach could provide new perspectives on the preparation of model metallosupramolecular architectures with desired functionalities.

Received: May 14, 2010

Published online: August 16, 2010

**Keywords:** gas separation · helical structures · metalloligands · microporous materials · supramolecular chemistry

- [1] For selected reviews, see: a) S. Horike, S. Shimomura, S. Kitagawa, *Nat. Chem.* **2009**, *1*, 695; b) R. A. Fischer, C. Wöll, *Angew. Chem.* **2008**, *120*, 8285; *Angew. Chem. Int. Ed.* **2008**, *47*, 8164; c) G. Férey, *Chem. Soc. Rev.* **2008**, *37*, 191; d) M. P. Suh, Y. E. Cheon, E. Y. Lee, *Coord. Chem. Rev.* **2008**, *252*, 1007; e) M. J. Zaworotko, *Nature* **2008**, *451*, 410; f) S. Kitagawa, R. Matsuda, *Coord. Chem. Rev.* **2007**, *251*, 2490; g) D. Bradshaw,

J. B. Claridge, E. J. Cussen, T. J. Prior, M. J. Rosseinsky, *Acc. Chem. Res.* **2005**, *38*, 273; h) J. L. C. Rowsell, O. M. Yaghi, *Microporous Mesoporous Mater.* **2004**, *73*, 3.

- [2] For selected reviews, see: a) D. Farrusseng, S. Aguado, C. Pinel, *Angew. Chem.* **2009**, *121*, 7638; *Angew. Chem. Int. Ed.* **2009**, *48*, 7502; b) J. Lee, O. K. Farha, J. Roberts, K. A. Scheidt, S. T. Nguyen, J. T. Hupp, *Chem. Soc. Rev.* **2009**, *38*, 1450; c) L. Ma, C. Abney, W. Lin, *Chem. Soc. Rev.* **2009**, *38*, 1248.
- [3] a) S. Ma, H.-C. Zhou, *Chem. Commun.* **2010**, *46*, 44; b) K. M. Thomas, *Dalton Trans.* **2009**, 1487; c) L. J. Murray, M. Dinca, J. R. Long, *Chem. Soc. Rev.* **2009**, *38*, 1315; d) R. E. Morris, P. S. Wheatley, *Angew. Chem.* **2008**, *120*, 5044–5059; *Angew. Chem. Int. Ed.* **2008**, *47*, 4966–4981; e) J. L. C. Rowsell, O. M. Yaghi, *Angew. Chem.* **2005**, *117*, 4748; *Angew. Chem. Int. Ed.* **2005**, *44*, 4670.
- [4] a) J.-R. Li, R. J. Kuppler, H.-C. Zhou, *Chem. Soc. Rev.* **2009**, *38*, 1477; b) D. Britt, D. Tranchemontagne, O. M. Yaghi, *Proc. Natl. Acad. Sci. USA* **2008**, *105*, 11623.
- [5] a) R. Robson, *J. Chem. Soc. Dalton Trans.* **2000**, 3735; b) O. M. Yaghi, M. O'Keeffe, N. W. Ockwig, H. K. Chae, M. Eddaoudi, J. Kim, *Nature* **2003**, *423*, 705; c) S. Kitagawa, R. Kitaura, S. Noro, *Angew. Chem.* **2004**, *116*, 2388; *Angew. Chem. Int. Ed.* **2004**, *43*, 2334; d) D. J. Tranchemontagne, J. L. Mendoza-Cortés, M. O'Keeffe, *Chem. Soc. Rev.* **2009**, *38*, 1257.
- [6] a) K. S. Suslick, P. Bhyrappa, J. H. Chou, M. E. Kosal, S. Nakagaki, D. W. Smithenry, S. R. Wilson, *Acc. Chem. Res.* **2005**, *38*, 283; b) S. R. Halper, L. Do, J. R. Stork, S. M. Cohen, *J. Am. Chem. Soc.* **2006**, *128*, 15255.
- [7] a) D. Braga, F. Grepioni, G. R. Desiraju, *Chem. Rev.* **1998**, *98*, 1375; b) A. M. Beatty, *Coord. Chem. Rev.* **2003**, *246*, 131; c) H. W. Roesky, M. Andruh, *Coord. Chem. Rev.* **2003**, *236*, 91; d) L. Brammer, *Chem. Soc. Rev.* **2004**, *33*, 476; e) S. Kitagawa, K. Uemura, *Chem. Soc. Rev.* **2005**, *34*, 109; f) M. R. Hosseini, *Acc. Chem. Res.* **2005**, *38*, 313.
- [8] a) D. V. Soldatov, J. A. Ripmeester, S. I. Shergina, I. E. Sokolov, A. S. Zanina, S. A. Gromilov, Yu. A. Dyadin, *J. Am. Chem. Soc.* **1999**, *121*, 4179; b) K. Yamada, S. Yagishita, H. Tanaka, K. Tohyama, K. Adachi, S. Kaizaki, H. Kumagai, K. Inoue, R. Kitaura, H. C. Chang, S. Kitagawa, S. Kawata, *Chem. Eur. J.* **2004**, *10*, 2647; c) S. U. Son, J. A. Reingold, G. B. Carpenter, D. A. Sweigart, *Chem. Commun.* **2006**, 708; d) S. A. Dalrymple, G. K. H. Shimizu, *J. Am. Chem. Soc.* **2007**, *129*, 12114; e) T. D. Nixon, L. D. Dingwall, J. M. Lynam, A. C. Whitwood, *Chem. Commun.* **2009**, 2890; f) R. Murugavel, S. Kuppaswamy, N. Gogoi, R. Boomishankar, A. Steiner, *Chem. Eur. J.* **2010**, *16*, 994.
- [9] a) A. I. Kitaigorodsky, *Molecular Crystals and Molecules*, Academic Press, New York, **1973**; b) C. P. Brock, J. D. Dunitz, *Chem. Mater.* **1994**, *6*, 1118.
- [10] For reviews, see: a) C. Kaes, A. Katz, M. W. Hosseini, *Chem. Rev.* **2000**, *100*, 3553; b) K. Biradha, M. Sarkar, L. Rajput, *Chem. Commun.* **2006**, 4169; c) S. A. Barnett, N. R. Champness, *Coord. Chem. Rev.* **2003**, *246*, 145.
- [11] T. Kaczorowski, I. Justyniak, T. Lipińska, J. Lipkowski, J. Lewiński, *J. Am. Chem. Soc.* **2009**, *131*, 5393.
- [12] R. Kumar, M. L. Sierra, J. P. Oliver, *Organometallics* **1994**, *13*, 4285.
- [13] Recently, these types of complexes generated in situ were examined in enantioselective catalytic processes: a) L. Liu, R. Wang, Y.-F. Kang, C. Chen, Z.-Q. Xu, Y.-F. Zhou, M. Ni, H.-Q. Cai, M.-Z. Gong, *J. Org. Chem.* **2005**, *70*, 1084; b) J. Shi, M. Wang, L. He, K. Zheng, X. Liu, L. Lin, X. Feng, *Chem. Commun.* **2009**, 4711.
- [14] Crystal data for **1**·THF: C<sub>42</sub>H<sub>54</sub>N<sub>4</sub>O<sub>2</sub>Al<sub>2</sub>·C<sub>4</sub>H<sub>8</sub>O, *M* = 772.96, monoclinic, space group *C*2 (no. 5), *a* = 16.4061(5), *b* = 15.2451(3), *c* = 17.4902(6) Å, β = 91.4400(10)°, *U* = 4373.0(2) Å<sup>3</sup>, *Z* = 2, *F*(000) = 1664, ρ<sub>calcd</sub> = 1.174 g cm<sup>-3</sup>, *T* = 100(2) K, *R*1 = 0.0598, *wR*2 = 0.1664 for 6547 reflections with

- $I_o > 2\sigma(I_o)$ ; crystal data for solvent-free **1**:  $a = 16.41$ ,  $b = 15.25$ ,  $c = 17.49$  Å,  $\beta = 95^\circ$ . The structure was solved by direct methods using the program SHELXS-97 and refined by full-matrix least squares on  $F^2$  using the program SHELXL-97. All non-hydrogen atoms were located by difference Fourier synthesis and refined anisotropically. All hydrogen atoms were included at geometrically calculated positions and refined by using a riding model. CCDC 758469 (**1**) contains the supplementary crystallographic data for this paper. These data can be obtained free of charge from The Cambridge Crystallographic Data Centre via [www.ccdc.cam.ac.uk/data\\_request/cif](http://www.ccdc.cam.ac.uk/data_request/cif).
- [15] For representative references, see: a) A. Willner, A. Hepp, N. W. Mitzel, *Dalton Trans.* **2008**, 6832; b) J. Lewiński, J. Zachara, I. Justyniak, *Chem. Commun.* **2002**, 1586; c) J. A. Francis, N. McMahon, S. G. Bot, A. R. Barron, *Organometallics* **1999**, *18*, 4399; d) M. P. Hogerheide, M. Wesseling, J. T. B. H. Jastrzebski, J. Boersma, H. Kooijman, A. L. Spek, G. van Koten, *Organometallics* **1995**, *14*, 4483.
- [16] The diameter corresponds to that of the largest probe atom, which can be fitted to the appropriate part of the channel based on the X-ray crystal structure. Calculated with Accelrys Materials Studio modeling software.
- [17] S. H. Jung, H.-K. Kim, J.-W. Yoon, J.-S. Chang, *J. Phys. Chem. B* **2006**, *110*, 9371.
- [18] W. Zhou, H. Wu, M. R. Hartman, T. Yildirim, *J. Phys. Chem. C* **2007**, *111*, 16131.
- [19] a) J. G. Vitillo, L. Regli, S. Chavan, G. Ricchiardi, G. Spoto, P. D. C. Dietzel, S. Bordiga, A. Zecchina, *J. Am. Chem. Soc.* **2008**, *130*, 8386; b) W. Zhou, H. Wu, T. Yildirim, *J. Am. Chem. Soc.* **2008**, *130*, 15268.
- [20] a) J.-P. Zhang, X.-M. Chen, *J. Am. Chem. Soc.* **2008**, *130*, 6010; b) H. Kim, D. G. Samsonenko, M. Yoon, J. W. Yoon, Y. K. Hwang, J.-S. Chang, K. Kim, *Chem. Commun.* **2008**, 4697.
- [21] We cannot, however, unambiguously exclude any significant structural changes responsible for the temperature-triggered N<sub>2</sub> adsorption effect because of the lack of diffraction data for guest-free **1** at low temperatures (77–293 K).
- [22] a) J.-B. Lin, J.-P. Zhang, X.-M. Chen, *J. Am. Chem. Soc.* **2010**, *132*, 6654; b) H. Wu, J. M. Simmons, Y. Liu, C. M. Brown, X.-S. Wang, S. Ma, V. K. Peterson, P. D. Southon, C. J. Kepert, H.-C. Zhou, T. Yildirim, W. Zhou, *Chem. Eur. J.* **2010**, *16*, 5205; c) P. L. Llewellyn, S. Bourrelly, C. Serre, A. Vimont, M. Daturi, L. Hamon, G. D. Weireld, J.-S. Chang, D.-Y. Hong, Y.-K. Hwang, S. H. Jung, G. Férey, *Langmuir* **2008**, *24*, 7245.
- [23] For examples, see: a) J. An, S. J. Geib, N. L. Rosi, *J. Am. Chem. Soc.* **2010**, *132*, 38; b) S. Couck, J. F. M. Denayer, G. V. Baron, T. Rémy, J. Gascon, F. Kapteijn, *J. Am. Chem. Soc.* **2009**, *131*, 6326; c) A. Demessence, D. M. D'Alessandro, M. L. Foo, J. R. Long, *J. Am. Chem. Soc.* **2009**, *131*, 8784.
- [24] A. L. Spek, *J. Appl. Crystallogr.* **2003**, *36*, 7.